Sains Malaysiana 46(2)(2017): 285–293
http://dx.doi.org/10.17576/jsm-2017-4602-13

Effects of Debinding and Sintering Atmosphere on Properties and Corrosion Resistance of Powder Injection Molded 316 L - Stainless Steel

(Kesan Pengikatan dan Pensinteran ke atas Sifat dan Rintangan Kakisan Acuan Suntikan Serbuk 316 L - Keluli Tahan Karat)

MUHAMMAD RAFI RAZA*, FAIZ AHMAD, NORHAMIDI MUHAMAD, ABU BAKAR SULONG, M.A. OMAR, MAJID NIAZ AKHTAR, MUHAMMAD ASLAM & IRFAN SHERAZI

ABSTRACT

316L stainless steel is a common biomedical material. Currently, biomedical parts are produced through powder injection molding (PIM). Carbon control is the most critical in PIM. Improper debinding can significantly change the properties of the final product. In this work, thermal debinding and sintering were performed in two different furnaces (i.e. laboratory and commercially available furnaces) to study the mechanical properties and corrosion resistance. Debounded samples were sintered in different atmospheres. The samples sintered in inert gas showed enhanced mechanical properties compared with wrought 316L stainless steel and higher corrosion rate than those sintered in the vacuum furnace. The densification and tensile strength of the hydrogen sintered samples increased up to 3% and 51%, respectively, compared with those of the vacuum-sintered samples. However, the samples sintered in inert gas also exhibited reduced ductility and corrosion resistance. This finding is attributed to the presence of residual carbon in debonded samples during debinding.

Keywords: Corrosion resistance; debinding; mechanical properties; powder injection molding; weight loss method

ABSTRAK

Keluli tahan karat 316L adalah bahan lazim bioperubatan. Pada masa ini, bahagian bioperubatan dihasilkan melalui acuan suntikan serbuk (PIM). Kawalan karbon adalah yang paling kritikal dalam PIM. Pengikatan sumbang boleh mengubah sifat akhir produk. Dalam kertas ini, pengikatan haba dan persinteran telah dijalankan di dua relau berbeza (Makmal dan relau yang tersedia secara komersial) untuk mengkaji sifat mekanik dan rintangan kakisan. Sampel terikat telah disinter dalam atmosfera berbeza. Sampel yang disinter dalam gas lengai yang menunjukkan peningkatan sifat mekanik berbanding dengan keluli tahan karat tempaan 316L dan kadar kakisan yang lebih tinggi berbanding yang disinter dalam vakum relau. Kepadatan dan kekuatan tegangan sampel hidrogen yang disinter meningkat masing-masing kepada 3% dan 51% berbanding dengan sampel yang disinter secara vakum. Walau bagaimanapun, sampel yang disinter dalam gas lengai juga menunjukkan pengurangan rintangan kemuluran dan kakisan. Keputusan kajian ini adalah kerana sifat sisa karbon dalam sampel ikatan semasa pengikatan.

Kata kunci: Acuan suntikan serbuk; kaedah kehilangan berat; rintangan kakisan; pengikatan; sifat mekanik

INTRODUCTION

Powder injection molding (PIM) is a low-cost technique used to fabricate high volumes of complex geometry parts with dimensional accuracy (Beebhas et al. 1995). PIM is also used to fabricate metal and ceramic parts (Zlatkov et al. 2008). PIM fabrication is performed in four consecutive steps, including feedstock preparation, injection molding, debinding and sintering (Raza et al. 2016). The feedstock is a mixture of metal powder and polymeric binders. Polymeric binders behave as a transporter to allow a metal powder to flow within the cavities and provide strength to molded parts for easy handling. Usually, low viscosity binders are recommended for PIM because these binders achieve optimum solid loading, uniform distribution of metal powder and ease of removal from molded parts (Zaky et al. 2009). A previous study utilized a palm-based binder system to produce 316L SS (stainless steel) parts; the SS parts exhibited sintered properties according to MPIF 35 standard (Omar et al. 2012). In another study, different binder systems, namely, PW-based and PEG-based binders were used to optimize debinding parameters, wherein large pores, which are helpful during thermal debinding, are formed during solvent extraction (Omar et al. 2003).

Another study investigated the effects of debinding on mechanical properties of 316L SS and found that control of carbon content during debinding affects the mechanical properties (Muhammad Rafi et al. 2013). In another study, the effects of debinding atmosphere were investigated; experiments showed that debinding rate is higher in vacuum than in hydrogen (H_2) atmosphere (Li et al. 2003). Researchers have studied the effects of various processing parameters such as binder composition (Huang et al. 2003), particle type (Khairur Rijal et al. 2008), debinding process (Muhammad Ilman et al. 2013), sintering temperature and

heating rate (Kurgan 2014; Loh et al. 2001), dwell time, pressure and atmosphere (Ji et al. 2001) on the densification and final mechanical properties of 316L SS.

Nowadays, metals such as Ti and Ti alloys, Co-Cr-alloys or stainless steel are widely used in medical industry. 316L stainless steel grade is recommended for medical applications because it exhibits several advantages that include low cost, excellent combination of mechanical properties and corrosion resistance, ease of availability and fabrication as compared to other alloys. A previous study of immersed PIM 316L SS parts in 3% NaCl solution for 78 days and found that 316L SS displayed pitting corrosion because of pores present in 316L SS (Sobral et al. 2001). Another study investigated the effects of sintering atmosphere on pitting corrosion resistance of 316L SS produced by powder metallurgy (PM); the authors found that vacuum sintering helped to attain high density and better corrosion resistance compared with gas sintering (García et al. 2008, 2007). In gas-sintered samples, lamellar components form. These components may reduce the corrosion resistance of materials. In another study, corrosion properties of AISI 316 austenitic stainless steel were investigated; this stainless steel was treated through active screen plasma nitriding (ASPN) (Li & Bell 2004). Corrosion was tested by measuring the weight loss of steel in acid and salt environments and the results showed that ASPN performed at low temperature (i.e. 450ºC) improved corrosion resistance because of formation of nitride layer at the surface (Li & Bell 2004). Corrosion degrades metallic implants. Corrosion rate depends on various factors, such as alloy composition, manufacturing technique and implant environment (Jamaludin et al. 2009). Ni and Cr are used in most metallic 316L SS medical implants. During the corrosion of 316L SS implants, Fe, Ni and Cr ions are released which can cause allergies and carcinogens. A previous study on retrieved implants showed that 90% of failures were due to corrosion attack (Hansen 2008).

The present study aimed to develop a range of formulations containing solid loadings from 60 to 69 vol%. It also investigated the effects of debinding and sintering atmosphere on properties and corrosion resistance of 316L SS. The molded test samples were debonded and sintered in vacuum (laboratory scale) and the test samples sintered in H_2, N_2 and mixture of N_2-H_2 atmospheres in commercial furnace. The sintered test samples are characterized in terms of densification, tensile strength measurements, morphology, measurement of toxic metal ions and corrosion resistance according to ASTM standards.

Experimental Details

Materials and Injection Molding

Commercial water atomized stainless steel 316L (PF-10R) was supplied by PACIFIC SOWA Japan. The measured mean particle size of the stainless steel was from 5 to 7 μm and the chemical composition of the powder provided by the supplier was according to ASTM standard F138-08.

Four feedstock formulations namely, F1, F2, F3 and F4, were prepared with solid loading of 60, 65, 67 and 69 vol%, respectively. Binder system consists of 70 vol% Paraffin wax, 25 vol% polypropylene and 5 vol% stearic acid. The stainless steel powder and wax-based binder were mixed using a Z-blade mixer with blade speed of 60 rpm at 180±5ºC for 90 min. The paste was dried and converted into granules after mixing. The test specimens were molded using a 100 KSA vertical injection molding machine according to MPIF standard 50. All formulations were molded at 180±5ºC and the molding dwell time was varied from 18-30 s, depending on the solid loading employed. Physical defects (i.e. cracks and trapped air) on the surface of the test samples were not observed.

Debinding was performed via two consecutive steps, namely, solvent extraction and thermal debinding. Solvent extraction was conducted by using a water circulating bath. The test specimens were heated to 450°C for 1 h at a heating rate of 7°C/min to remove the remaining binder produced during thermal debinding (Rafi Raza et al. 2012; Raza et al. 2012). Vacuum sintering was accomplished by conducting the thermal debinding in a high-temperature furnace (HT-Type 1400-M). Meanwhile, atmospheric gas sintering was achieved by using a commercially available high-temperature production furnace (HTPF) for thermal debinding and sintering. The test samples debonded in the HT-type 1400-M furnace were sintered in a vacuum with graphite-heating element furnace at 1325°C for 2 h (dwell time). The samples were post-sintered at a cooling rate of 3°C/min. Meanwhile, the test samples debonded in the HTPF commercial furnace were also sintered at 1325°C for 2 h (dwell time) and post-sintered at a cooling rate of 3°C/min in H_2, N_2 and mixture of H_2/N_2 (9:1). These procedures were performed to investigate the effects of atmospheric sintering on densification, mechanical properties and corrosion resistance of the PIM 316L SS test samples.

Characterization of Sintered Samples

The density of the sintered test samples was measured through a water immersion technique. The tensile strength of the samples was determined in accordance with the ASTM standard method E8M-00 using Amsler 100 (Zwick/Roell). C content in the sintered test samples was determined in accordance with ASTM standard E1019. The morphology and elemental content of the test samples sintered in different furnaces were determined. Selected samples from each batch of formulation were analyzed using FE-SEM and EDX after immersing the samples for 30 days in simulated body solution (i.e. Ringer's solution). Corrosion exhibited by the test samples was measured by preparing the samples in accordance with ASTM standards G-01. Weight loss method was used to study the corrosion behavior of the sintered test samples. The test specimens were immersed in a simulated body solution (i.e. Ringer's solution at 37±1°C for 30 days) and the pH of the solution was maintained at 7.4 by using 1 M HNO_3 or 1 M NaOH. After completing the weight loss test, the solutions were

analyzed by atomic absorption spectroscopy to determine the metal ion concentrations in the samples.

Results and Discussion

Effects of Sintering Atmosphere on Density

The F2 formulation with a solid loading of 65 vol% attained 97% of theoretical density in H_2 sintering and 94% in vacuum sintering, respectively, as shown in Figure 1.

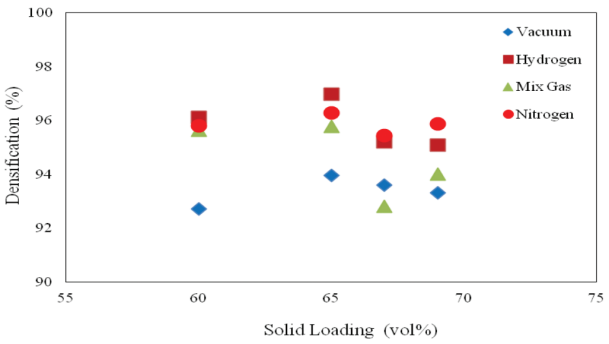

FIGURE 1. Effects of sintering atmosphere on densification of PIM 316L stainless steel

The F2 formulation samples debonded and sintered in H_2 using a commercial furnace exhibited 3% higher sintered density than the vacuum-sintered samples using laboratory facilities. The difference in densities is attributed to the residual 'C' produced during thermal debinding; this residual 'C' enhanced the sintering rate to achieve the maximum density (Levenfeld et al. 2002). The samples with solid loadings greater than 65 vol% exhibited decreased sintered density, which could be due to solid loadings that were above the critical value. Increased solid loading above the critical value resulted in reduced sintered density because of the presence of pores within the molded samples (German & Bose 1997). The sintered test samples with no residual 'C' from debinding showed a smooth surface, whereas the test samples with 'C' content and sintered in gas displayed a rough surface which was confirmed in our published research (Raza et al. 2015). This finding could be due to the formation of carbides at the surface and within the matrix during carburization (Eisenhüttenleute 1992). The presence of carbide and nitride in the gas-sintered test samples were confirmed through XRD in our previous study (Muhammad Rafi et al. 2013), which showed the presence of additional carbide and nitride phases other than the austenite phase.

Effects of Sintering Atmosphere on Mechanical Properties

The results in Figure 2 shows the comparison of mechanical properties where formulation with solid loading of 65 vol% (F2) exhibited maximum tensile strength in all atmospheres. The maximum tensile strength measured for the 65 vol% solid loading was 484 MPa for the test samples sintered in vacuum. Meanwhile, the tensile strength increased by 31% and 51% in the H_2 and N_2 atmosphere, respectively. This may be attributing due to the presence of carbon and atmosphere. Other formulations showed less tensile strength because the powder loading is above and below the critical loading which was responsible of abnormal behavior.

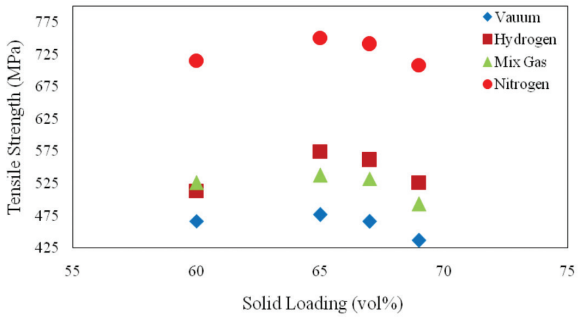

FIGURE 2. Effects of sintering atmosphere on tensile strength of PIM 316L SS

Figure 3 shows that the samples sintered in inert atmospheres lost their ductility. This finding can be attributed to the presence of residual carbon that formed during debinding and the slow cooling rate employed. During the cooling process, carbon reacted with the metal elements, namely, Fe and Cr and formed carbides and nitrides at the surface and across the grain boundaries; carbides and nitrides cause the brittleness of the material during the cooling process (Beachem 1972; Eliezer 1983; Levenfeld et al. 2002; Eisenhüttenleute 1992). Figure 3(b) and 3(c) shows the presence of slip planes, which indicate the nature of the brittle fracture in the samples. The samples with solid loading is greater than 65 vol% exhibited decreased tensile strength. This behavior is attributed to the presence of pores in the sample; porosity forms when solid loading is greater than the critical value; in this condition, tensile strength ultimately decreases (German & Bose 1997).

The fractures were dimples in nature; however, a high resolution of the crystalline facture across the grain boundaries was observed, as labelled in Figure 3(c) and 3(d). This finding indicates that sintering in N_2 atmosphere improved the mechanical properties of 316L SS as compared to vacuum sintering and the samples showed transition properties between ductile and brittle (Hua-bing Li et al. 2009; Montasser Marasy Dewidar et al. 2006). The improvement may be due to the formation of nitrides, as mentioned earlier, which was confirmed from the XRD analysis in a previous work (Muhammad Rafi et al. 2013). The formation of nitrides can be prevented by increasing the post-sintering cooling rate to approximately 200°C/min (Montasser Marasy Dewidar et al. 2006). Therefore, the effects of N_2 sintering on mechanical properties and microstructure is still unknown (Bostjan et

al. 2006). Furthermore, the N_2-sintered samples showed less brittleness compared with the H_2-sintered samples. The tensile strength achieved in this study were comparable with that of wrought 316L SS (according to ASTM standard) (Becker et al. 2000).

EFFECTS OF RESIDUAL CARBON ON SURFACE MORPHOLOGY

FESEM examination of the vacuum-sintered test samples (F2) showed that the Cr oxide layer at the surface was destroyed in a chloride environment (i.e. Ringer's Solution) as shown in Figure 4. This finding is due to the diffusion of more Cr atoms and long reaction time of the Cr atoms during cooling, which allowed the Cr atoms to react with carbon to form chromium carbides. As a result, less Cr atoms were left at the surface of the test sample; small particles (Cr_2O_3) were also distributed because of this reason. Figure 4 shows the result of EDX analysis, which confirmed the result obtained from FE-SEM. The formation of Cr oxide is probably due to the presence of O in the sample. EDX analysis of the sample surface showed the presence of 'C' from 0.35 to 1.5%, which is possibly due to the use of the graphite-heating element furnace or the small amount of residual carbon from the binder produced during thermal debinding. Carbon content was also measured through wet analysis (Table 1) after sintering.

The 'C' formed carbides because of the slow cooling rate of 3°C/min. Some pores were found at the surface of the samples, indicating that corrosion occurred; corrosion attack occurred because of the oxide layer, which was not enriched with metal oxide (Cr_2O_3). Chloride ions easily destroyed the oxide layer and caused pitting corrosion, which led to localized corrosion attack. By comparing the densification results, we conclude that porosity decreased when the solid loading below the critical solid loading was increased as clear in Figure 1. Pin-hole porosity leads to corrosion attack, as observed in Figure 4.

Figures 5 and 6 present the surface morphology of the test samples sintered in H_2 alone and mixture of H_2 and N_2, respectively. Both micrographs show needle-like structure on the surface of the sintered samples. These needles were identified as Cr carbides through EDX analysis. Although the Cr oxide layer was formed from the reaction of O_2 with Cr, the oxide layer was not enough to terminate

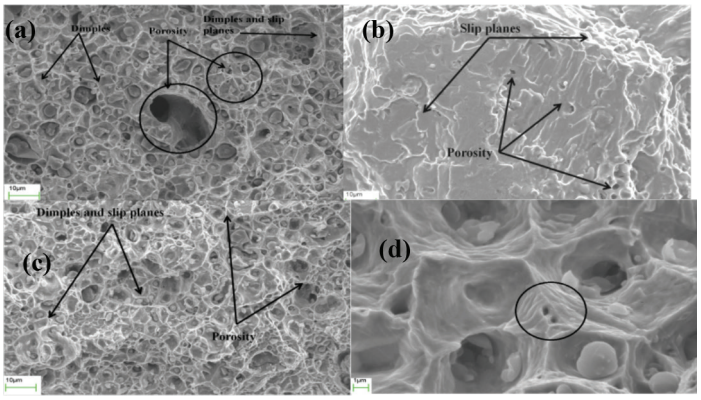

FIGURE 3. Tensile fractures of 316L SS (F2) sintered in (a) vacuum, (b) H_2, (c) N_2 and H_2 and (d) N_2 at 1325°C

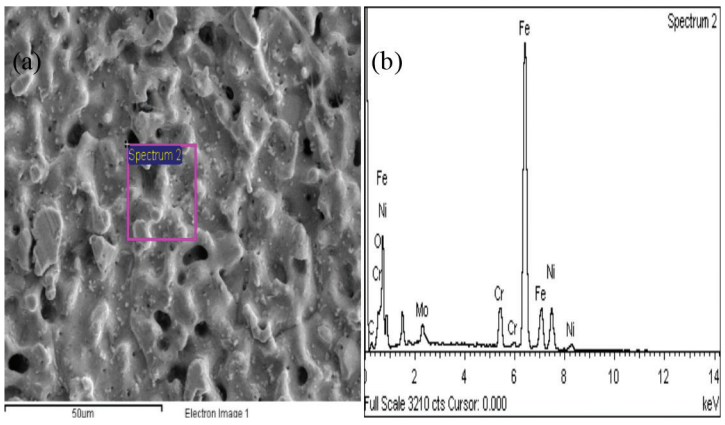

FIGURE 4. FESEM micrograph and corresponding EDX result of vacuum-sintered 316L SS at post-sintering cooling rate of 3°C/min showing the pores and Cr_2O_3 particles; (a) morphology and (b) EDX spectrum

TABLE 1. Carbon content measured using ASTM E1019 in sintered test samples (F2)

Atmosphere	% Carbon
Vacuum	0.00636
H_2	1.4955
Mixture of H_2&N_2	1.3215
N_2	0.1392

the corrosion attack. Both morphologies show that these carbides were uniformly distributed at the surface of the samples. These carbides that formed because of slow cooling rate behaved as corrosion initiators. The presence of white spots at surface represented the chlorides present in the sample.

The carbides formed during sintering promoted the formation of pin-holes at the surface; thus, corrosion was initiated. The formation of carbides is due to the improper thermal debinding, followed by a slow post-sintering cooling rate (Levenfeld et al. 2002). The presence of cracks also indicated the presence of stresses at the surface of the sintered samples and along the grain boundaries as shown in Figure 5(a), which were generated because of the presence of carbides in H_2 atmosphere (Eliezer 1983). The presence of carbides also indicated the presence of stresses at the surface of the sintered samples and along the grain boundaries. The diffusion of H_2 and N_2 at the surface during sintering; a concrete explanation is not available as the behavior of the N_2 is still unknown (García et al. 2007).

Figure 7 shows the morphology and EDX analysis, wherein C and N_2 were uniformly distributed within the

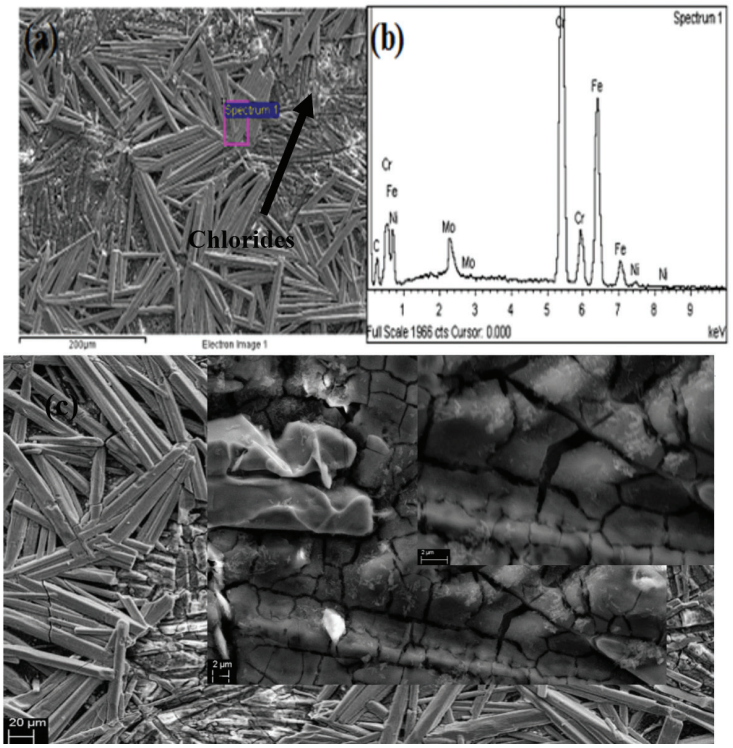

FIGURE 5. EDX analysis of H_2 sintered PIM 316L SS (F1) at 1325°C showing the carbides and cracks; (a) morphology of the corroded samples (b) EDX spectrum and (c) morphology showing cracks at the surface

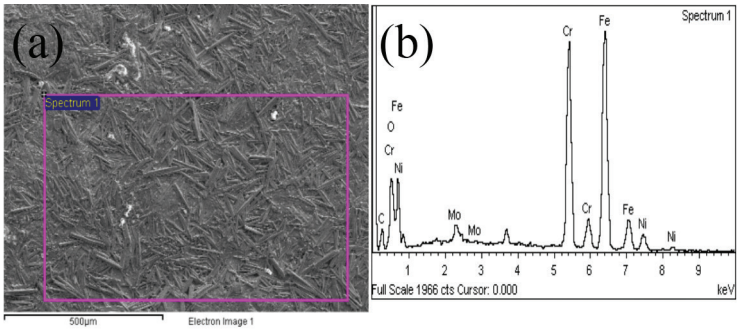

FIGURE 6. EDX analysis of PIM 316L SS (F2) sintered at 1325°C in H_2/N_2; (a) rod-like morphology at surface and (b) EDX spectrum

matrix. This condition improved the corrosion resistance in a chloride environment. N_2 was observed at the surface of the test samples sintered in N_2, which was dissolved within the matrix and formed nitrides; this observations were confirmed through XRD (Muhammad Rafi et al. 2013). N_2 may have a significant role in the dissolution of carbides within the matrix and at the surface of the sample. García et al. (2007) have mentioned that this type of structure is due to the mixture of Cr_2N and austenitic alloy in the presence of high-pressure N_2 atmosphere. Dissolving the carbides may have enhanced the corrosion resistance in the same way, as observed in the vacuum-sintered samples.

EFFECTS OF SINTERING ATMOSPHERE ON CORROSION BEHAVIOR OF 316L SS

The test samples sintered in all atmospheres were immersed in Ringer's solution for 30 days. Figure 8 shows the results of the corrosion measurement of the sintered test samples in different atmospheres. The vacuum-sintered test samples showed minimum pitting corrosion attack (corrosion rate) compared with the gas-sintered test samples. This result may be due to the presence of carbides, which formed because of the reaction between residual C from thermal debinding and Ni and Cr from sintering. The FESEM results showed that the presence of carbides which may be the one of the reason to increase the pitting corrosion attack. Pitting corrosion occurred because chlorides were present in the simulated body solution. Relatively less corrosion was observed in the vacuum-sintered samples immersed in Ringer's solution, which is probably due to the low evaporation of Cr ion during sintering. The Cr ions settled on the surface of the test samples and formed a passive oxide layer that protected the samples from corrosion in a chloride environment (Trepanier et al. 2000; Rafi Raza et al. 2012). The N_2-sintered samples exhibited a higher corrosion rate than the vacuum-sintered samples; however, the corrosion rate of the N_2-sintered samples was less than that of the H_2-sintered samples. It may be due to the fact that presence of H_2 minimized the formation of chromium oxide. In contrast to carbides, the presence of nitrides at the sample surface reduced corrosion by decreasing the number of open pores and dissolving the N_2 gas within the matrix, which improved corrosion resistance (García et al. 2007; Martin et al. 2014). These observations were confirmed by the results of the weight loss measurements and atomic absorption analysis.

Table 2 illustrates the detailed results obtained from AAS. More metal ions were released from the gas-sintered samples compared with those in the vacuum-sintered samples. This finding is possibly due to the presence of carbides and nitrides at the surface of the sintered samples that hindered the formation of a Cr oxide layer, which caused the release of more metal ions. Table 2 also shows the trace analysis of the Ringer's solution after measuring

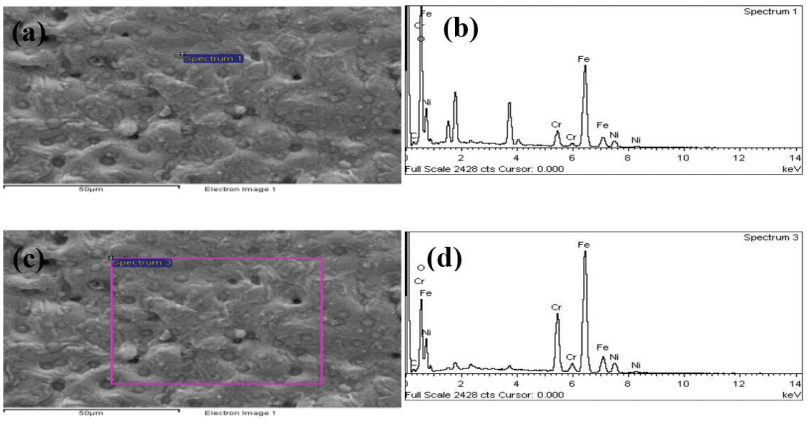

FIGURE 7. EDX analysis of PIM 316L SS (F2) sintered in N_2, (a) morphology of the corroded sample, (b) EDX, (c) morphology and (d) EDX spectrum

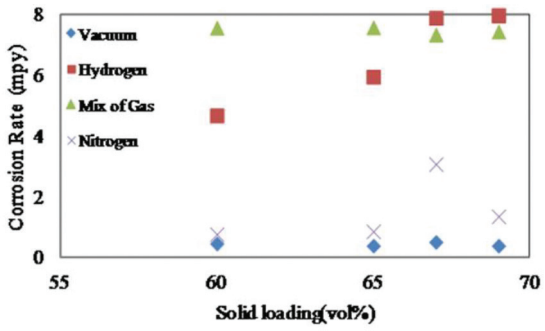

FIGURE 8. Effects of atmosphere on corrosion resistance of PIM 316L SS

TABLE 2. Contents of trace elements in solution after corrosion test

Formulation (vol%)	Vacuum			Hydrogen			Mix of gases			Nitrogen		
	Ni	Cr	Fe	Ni	Cr	Fe	Ni	Cr	Fe	Ni	Cr	Fe
60	0.0021	0.0011	0.0049	0.0074	0.0005	0.0054	0.0128	0.0002	0.0476	0.0125	0.05	0.0398
65	0.00056	0.0002	0.00084	0.0022	0.0002	0.0071	0.0136	0.0002	0.1268	0.0111	0.01	0.0276
67	0.001	0.0002	0.0014	0.068	0.0004	0.0208	0.0234	0.0004	0.123	0.0167	0.03	0.0318
69	0.002	0.0009	0.0018	0.0045	0.0045	0.0158	0.0051	0.0003	0.0312	0.0222	0.02	0.0827

* ppm unit for metal ions

the weight loss of the samples. Significant amounts of Ni, Cr and Fe were detected in the solutions of the gas-sintered samples. The release of ions from the surface of the vacuum-sintered parts was in the following order: Fe, Ni and Cr. These released ions were less than the obtained results in gas sintering atmospheres. Moreover, elements, such as Cr, formed an oxide layer that protected the sample against corrosion attack in a chloride environment; this condition was observed during the post-sintering cooling process. The F2 formulation showed low release of ions among all of the vacuum-sintered formulations. This result is attributed to the formation of Cr oxide particles at the surface of the part and high density of the formulation, which affected the reduction of open pores compared with the other formulations. These factors may have reduced the corrosion attack and lessened the release of metal ions. However, a fundamental relationship relating the release of ions with corrosion rate is not available.

The release of ions are higher in the test sample sintered in gas atmosphere that those in the vacuum-sintered samples. This finding can be attributed to the formation of carbides by residual carbon produced during debinding. In addition, the presence of H_2 hindered the formation of an oxide layer (Davis 1994), thereby resulting in increased corrosion rate. The same behavior was observed for the samples sintered in the mixed-gas atmosphere.

The behavior of N_2 is still not clearly understood. N_2 atoms clearly diffused within the matrix and formed nitrides, which may help dissolve the carbide and form nitride. N_2 may have terminated the release of metal ions in a chloride environment. The N_2-sintered samples released higher amounts of metal ions than the samples sintered in H_2.

CONCLUSION

Based on the results, we can conclude that residual carbon was present in the samples debonded in a commercial furnace which significantly improved the final properties of the PIM 316L SS parts; however, the corrosion resistance of the samples decreased. The results showed that vacuum-sintered samples exhibited a maximum densification of 94% whereas the samples sintered in H_2 atmosphere showed a maximum densification of 97% with the same formulation (F2). This result is attributed to the presence of residual C produced during debinding. While F2 formulation sintered in N_2 showed increased tensile strength up to 51% as compared with the vacuum-sintered samples; however, the ductility of the sample sintered in N_2 was reduced to 15%. It is concluded that vacuum sintered atmosphere is helpful to enhance the corrosion resistance and minimize the release of metal ions in chloride environment.

ACKNOWLEDGEMENTS

The authors wish to thank Universiti Teknologi PETRONAS, Advanced Materials Research Centre (AMREC) SIRIM, Malaysia and UKM-ICONIC-2013-003 and UKM- DIP-2012-29 for providing the funds and laboratory facilities.

REFERENCES

Beachem, C.D. 1972. A new model for hydrogen-assisted cracking (hydrogen embrittlement). *Metallurgical Transactions* 3: 441-455.

Becker, B.S., Boltom, J.D. & Eagles, A.M. 2000. Sintering of 316L stainless steels to high density via the addition of chromium-molybdenum dibromide powders Part 1: Sintering performance and mechanical properties. *Proceedings of the Institution of Mechanical Engineers. Part L, Journal of materials, design and applications, LHL*. pp. 139-152.

Beebhas, C., Mutsuddy, Ford, R.G. 1995. *Ceramic Injection Molding*. London: Chapman & Hall.

Bostjan Berginc, Zlatko Kampus & Borivoj Sustarsic. 2006. The influence of MIM and sintering-process parameters on the mechanical properties of 316L SS. *Materiali in Tehnologije* 40: 193-198.

Davis, J.R. 1994. *Stainless Steels*. West Conshohocken, PA: ASTM International.

Dewidar, M.M., Yoon, H-C. & Lim, J.K. 2006. Mechanical properties of metals for biomedical applications using powder metallurgy process: A review. *Metals and Materials* 12: 193-206.

Eisenhüttenleute, V.D. 1992. *Steel - A Handbook for Materials Research and Engineering: Volume 1: Fundamentals*. 1st ed. New York: Springer.

Eliezer, D. 1983. The behaviour of 316L stainless steel in hydrogen. *Journal of Materials Science* 18: 1540-1547.

García, C., Martín, F., Tiedr, P.d., Blanco, Y., Ruíz-Roman, J.M. & Aparicio, M. 2008. Electrochemical reactivation methods applied to PM austenitic stainless steels sintered in nitrogen-hydrogen atmosphere. *Corrosion Science* 50: 687-697.

García, C., Martín, F., Tiedra, P.d. & Garcia Cambronero, L. 2007. Pitting corrosion behaviour of PM austenitic stainless steels sintered in nitrogen-hydrogen atmosphere. *Corrosion Science* 49: 1718-1736.

German, R.M. & Bose, A. 1997. Powder injection molding of metal and ceramics. In *Metal Powder Industries Federation*. New Jersey: Princeton Press.

Hansen, D.C. 2008. Metal corrosion in the human body: The ultimate bio-corrosion scenario. *Electrochem. Soc. Interface* 17: 31-34.

Huang, B., Liang, S. & Qu, X. 2003. The rheology of metal injection molding. *Journal of Materials Processing Technology* 137: 132-137.

Li, H.B., Jiang, Z.H., Cao, Y. & Zhang, Z.R. 2009. Fabrication of high nitrogen austenitic stainless steels with excellent mechanical and pitting corrosion properties. *International Journal of Minerals, Metallurgy and Materials* 16: 387-392.

Li, Y., Liu, S., Qu, X. & Huang, B. 2003. Thermal debinding processing of 316L stainless steel powder injection molding compacts. *Journal of Materials Processing Technology* 137: 65-69.

Jamaludin, K.R., Muhamad, N., Ab-Rahman, M.N., M. Amin, S.Y., Ahmad, S., Ibrahim, M.H.I. 2009. Sintering parameter optimization of the SS316L metal injection molding (MIM) compacts for final density using taguchi method, *3rd South East Asian Technical University Consortium*, Johor Bahru, Malaysia, pp. 258-262.

Ji, C.H., Loh, N.H., Khor, K.A. & Tor, S.B. 2001. Sintering study of 316L stainless steel metal injection molding parts using Taguchi method: Final density. *Materials Science and Engineering* Vol. A (311): 74-82.

Khairur Rijal Jamaludin, Norhamidi Muhamad, Mohd Nizam Ab Rahman, Sri Yulis M. Amin, Sufizar Ahmad, Mohd Halim Irwan Ibrahim, Murtadhahadi & Nor Hafiez Mohamad Nor. 2008. Densification of ss316l gas-atomized and water-atomized powder compact, *Seminar II - AMReG* 08, Port Dickson. p. 8.

Kurgan, N. 2014. Effect of porosity and density on the mechanical and microstructural properties of sintered 316L stainless steel implant materials. *Materials & Design* 55: 235-241.

Levenfeld, B., Varez, A. & Torralba, J.M. 2002. Effect of residual carbon on the sintering process of M2 high speed steel parts obtained by a modified metal injection molding process. *Metallurgical and Materials Transactions A* 33: 1843-1851.

Li, C.X. & Bell, T. 2004. Corrosion properties of active screen plasma nitrided 316 austenitic stainless steel. *Corrosion Science* 46: 1527-1547.

Loh, N.H., Tor, S.B. & Khor, K.A. 2001. Production of metal matrix composite part by powder injection molding. *J. Mat. Processing Tech.* 108: 398-407.

Martin, F., García, C., Blanco, Y. & Herranz, G. 2014. Influence of sinter-cooling rate on intergranular corrosion of powder metallurgy superaustenitic stainless steel. *Corrosion Engineering, Science and Technology* 49: 614-623.

Muhammad Ilman Hakimi Chua, Abu Bakar Sulong, Mohd. Fazuri Abdullah & Muhamad, N. 2013. Optimization of injection molding and solvent debinding parameters of stainless steel powder (SS316L) based feedstock for metal injection molding. *Sains Malaysiana* 42(12): 1743-1750.

Muhammad Rafi Raza, Faiz Ahmad, Omar, M.A., German, R.M. & Ali S. Muhsan. 2013. Role of debinding to control mechanical properties of powder injection molded 316L stainless steel. *Advanced Materials Research* 699: 875-882.

Omar, M., Subuki, I., Abdullah, N., Zainon, N.M. & Roslani, N. 2012. Processing of water-atomised 316L stainless steel powder using metal injection processes. *Journal of Engineering Science* 8: 1-13.

Omar, M.A., Ibrahim, R., Sidik, M.I., Mustapha, M. & Mohamad, M. 2003. Rapid debinding of 316L stainless steel injection moulded component. *Journal of Materials Processing Technology* 140: 397-400.

Rafi Raza, M., Faiz Ahmad, Omar, M.A. & German, R.M. 2012. Effects of cooling rate on mechanical properties and corrosion resistance of vacuum sintered powder injection molded 316 L stainless steel. *Journal of Materials Processing Technology* 212: 164-170.

Raza, M.R., Ahmad, F., Muhamad, N., Sulong, A.B., Omar, M., Akhtar, M.N. & Aslam, M. 2016. Effects of solid loading and cooling rate on the mechanical properties and corrosion behavior of powder injection molded 316 L stainless steel. *Powder Technology* 289: 135-142.

Raza, M.R., Ahmad, F., Muhamad, N., Sulong, A.B., Omar, M., Akhtar, M.N., Nazir, M.S., Muhsan, A.S. & Aslam, M. 2015. *Effects of Residual Carbon on Microstructure and Surface Roughness of PIM 316L Stainless Steel, InCIEC 2014*. New York: Springer. pp. 927-935.

Raza, M.R., Ahmad, F., Omar, M., German, R. & Muhsan, A.S. 2012. Defect analysis of 316LSS during the powder injection moulding process, defect and diffusion forum. *Trans Tech Publ.* 329: 35-43.

Sobral, A.V.C., Ristow, Jr. W., Azambuja, D.S., Costa, I. & Franco, C.V. 2001. Potentiodynamic tests and electrochemical impedance spectroscopy of injection molded 316L steel in NaCl solution. *Corrosion Science* 43: 1019-1030.

Trepanier, C., Ramakrishna Venugopalan & Pelton, A.R. 2000. Corrosion resistance and biocompatibility of passivated NiTi. In *Shape Memory Implants,* edited by Yahia, L. New York: Springer Berlin Heidelberg. pp. 35-45.

Zaky, M.T., Soliman, S. & Farag, S. 2009. Influence of paraffin wax characteristics on the formulation of wax-based binders and their debinding from green molded parts using two comparative techniques. *Journal of Materials Processing Technology* 209: 5981-5989.

Zlatkov, B.S., Griesmayer, E., Loibl, H., Danninger, H. & Gierl, C. 2008. Recent advances in PIM technology I. *Science of Sintering* 40: 79-88.

Muhammad Rafi Raza* & Irfan Sherazi
Department of Mechanical Engineering
COMSATS Institute of Information Technology Sahiwal
Pakistan

Faiz Ahmad
Department of Mechanical Engineering
Universiti Teknologi PETRONAS
32610 Bandar Seri Iskandar, Perak Darul Ridzuan
Malaysia

Norhamidi Muhamad & Abu Bakar Sulong
Department of Mechanical and Materials Engineering
Universiti Kebangsaan Malaysia
43600 UKM Bangi, Selangor Darul Ehsan
Malaysia

M.A. Omar
Advanced Materials Research Centre (AMREC) SIRIM
Kulim Hi-Tech Park
09000 Kulim, Kedah Darul Aman
Malaysia

Majid Niaz Akhtar
Department of Physics
COMSATS Institute of Information Technology Lahore
Pakistan

*Corresponding author; email: rafirazamalik@gmail.com

Received: 13 June 2015
Accepted: 11 May 2016